

RESEARCH

Open Access



The role of IGF2BP2 in macrophage-mediated NLRP3 inflammasome activation in the pathogenesis of dry AMD

Yuqing Zhao^{1,2,3,4}, Yu Zhang^{1,2,3,4}, Junfang Li^{1,2,3,4}, Yifei Zhang^{1,2,3,4} and Yi Qu^{1,2,3,4*}

Abstract

Background Dry age-related macular degeneration (AMD) is a common chronic degenerative eye disease for which there is currently no effective treatment. Insulin-like growth factor 2 mRNA-binding protein 2 (IGF2BP2) is a recently identified m6A reader that binds RNA and maintains its stability, thereby participating in various biological processes. However, its role in dry AMD remains unclear.

Methods In this study, we investigated the role of IGF2BP2 in macrophage NLRP3 inflammasomes using a sodium iodate-induced dry AMD model.

Results Our results demonstrated that IGF2BP2 is highly expressed in the retinal-choroidal tissue induced by sodium iodate, with its effects primarily occurring in macrophages. The loss of IGF2BP2 ameliorating dry AMD. Mechanistically, methylated NLRP3 transcripts were subsequently directly recognized by the specific m6A “reader”, IGF2BP2, to prevent NLRP3 mRNA degradation. Furthermore, in vivo experiments, to maintain the eye’s “immune privilege”, we employed mesoporous silica-based cell therapy to target and regulate macrophage IGF2BP2, providing a foundation for the evaluation and translation of therapies targeting this gene.

Conclusion our study reveals that the molecular mechanism of dry AMD pathogenesis involves IGF2BP2-mediated NLRP3 inflammasome activation in macrophages, highlighting IGF2BP2 as a promising biomarker and therapeutic target for dry AMD treatment.

Keywords Dry Age-Related macular degeneration, IGF2BP2, M6A reader, Macrophages, NLRP3

Introduction

Age-related macular degeneration (AMD) primarily occurs in the elderly and is a leading cause of progressive visual impairment and vision loss [1]. Dry (nonexudative) and wet (neovascular) are the two forms of macular degeneration. Clinically, dry AMD is the most common form, accounting for 90% of AMD cases. Although the progression of dry AMD is typically slow, it can eventually lead to geographic atrophy (GA) or convert to wet AMD, resulting in irreversible vision loss. While various treatment options are available for wet AMD, effective therapies for dry AMD remain lacking [2–4]. Given the

*Correspondence:

Yi Qu

yiqucn@sdu.edu.cn

¹Department of Geriatrics, Qilu Hospital of Shandong University, No. 107, Wenhuxi Road, Jinan 250012, China

²Key Laboratory of Cardiovascular Proteomics of Shandong Province, Jinan, China

³Jinan Clinical Research Center for Geriatric Medicine (202132001), Jinan, China

⁴Department of Ophthalmology, Qilu Hospital of Shandong University, Jinan, China



© The Author(s) 2025. **Open Access** This article is licensed under a Creative Commons Attribution-NonCommercial-NoDerivatives 4.0 International License, which permits any non-commercial use, sharing, distribution and reproduction in any medium or format, as long as you give appropriate credit to the original author(s) and the source, provide a link to the Creative Commons licence, and indicate if you modified the licensed material. You do not have permission under this licence to share adapted material derived from this article or parts of it. The images or other third party material in this article are included in the article's Creative Commons licence, unless indicated otherwise in a credit line to the material. If material is not included in the article's Creative Commons licence and your intended use is not permitted by statutory regulation or exceeds the permitted use, you will need to obtain permission directly from the copyright holder. To view a copy of this licence, visit <http://creativecommons.org/licenses/by-nc-nd/4.0/>.

lack of effective treatments for this condition, there is an urgent need to better understand the molecular mechanisms driving AMD pathogenesis and to identify potential targets as clues for developing effective therapies.

Inflammation is a key pathogenic factor in dry AMD [5]. Evidence suggests that the accumulation and activation of macrophages have been detected in the retinal lesions of patients with dry AMD [6–8]. Research indicates that macrophages with inflammatory effects can inflict both sublethal and lethal damage to RPE cells and photoreceptors, thereby contributing directly to the progression of AMD [9, 10]. Notably, during the progression of dry AMD, the NOD-like receptor protein 3 (NLRP3) inflammasome exhibits excessive activation in macrophages [11, 12]. The NLRP3 inflammasome is a multi-protein complex in the cytoplasm that participates in the production of pro-inflammatory cytokines, including caspase-1 and the crucial IL-1 β , which is believed to play a major role in retinal degeneration [13, 14]. Thus, regulating macrophage-mediated retinal inflammation has emerged as a promising therapeutic strategy for treating dry AMD.

N6-methyladenosine (m6A) is the most common and abundant internal modification in eukaryotic messenger RNAs [15–17]. Increasing evidence suggests that m6A modification is involved in the expression and activation of the NLRP3 inflammasome in macrophages. Zhou et al. found that exosomes derived from human umbilical cord mesenchymal stem cells alleviated the progression of osteoarthritis in mice by binding to METTL3 and reducing the m6A levels of NLRP3 mRNA in macrophages [18]. Similarly, Hao et al. discovered that YTHDF1 promotes the production of pro-inflammatory IL-1 β in macrophages during bacterial infection in a sepsis mouse model [19]. A recently identified family of m6A readers is the IGF2BPs family, consisting of IGF2BP1, IGF2BP2, and IGF2BP3. These proteins recognize and bind to m6A-modified mRNA. IGF2BP2 plays an important role in various biological processes, including cancer progression and inflammatory diseases [20, 21]. Remarkably, Wang et al. made an innovative contribution by elucidating how IGF2BP2 in macrophages regulates the transition between M1 and M2 polarization through m6A modification [22]. This discovery offers a strong theoretical foundation for investigating the potential involvement of IGF2BP2 in inflammatory diseases. Nevertheless, the role of IGF2BP2 as an m6A reader in the context of dry AMD has not yet been reported.

In this study, we found that IGF2BP2 expression by macrophages plays an unexpected role in the progression of dry AMD. We further uncovered a novel mechanism of dry AMD via m6A-IGF2BP2/NLRP3-dependent way in macrophages. Additionally, we utilized mesoporous silica nanoparticles (MSN) as a drug delivery system.

Based on this, we developed folic acid-modified nanoparticles (FA-MSN-CWI1-2) loaded with the IGF2BP2 inhibitor CWI1-2 to effectively target activated macrophages, thereby achieving conditional downregulation of IGF2BP2 in intraocular macrophages.

Method

Animals

IGF2BP2-deficient mice were provided by Shanghai Southern Model Biotechnology, among them, littermate mice with matched age and gender were included in all experiments in the study. All animals were raised under certain pathogen-free conditions (Qilu Hospital, Shandong University). All experiments obtained the approval of the Laboratory Animal Ethics and Welfare Committee of Qilu Hospital of Shandong University (approval No.: DWLL-2024–166).

Clinical investigation and histopathology

Optical coherence tomography (OCT; RTVue XR Avanti, Optovue) together with color fundus imaging (Daytona, Optos) were adopted for the evaluation of anesthetized mice' *in vivo* retinal lesions prior to drug administration and seven days after the sodium iodate modeling, respectively. Then, mice were placed in dark environment for one night to achieve dark adaption. Flash electroretinogram (ERG) also followed the abovementioned procedures [23]. A Visual Electrophysiological Monitor system (#RetiMINER-C ERG, IRC, Chongqing, China) served for the FERG measurement.

The eyeballs of euthanized mouse underwent 24 h of fixation in FAS eyeball fixative (Servicebio, Wuhan, China), and then paraffin embedding. Samples were sectioned into 4- μ m-thick slices, with their pathological alternation being tested based on the TUNEL and H&E staining. Subsequently, paraffin sections were subjected to immunofluorescence staining with antibodies against NLRP3 (1:500, Servicebio, Jinan, China) and F4/80 (1:500, Servicebio). Image analysis relied on a fluorescence microscope together with a light microscope.

TUNEL staining

Paraffin sections were deparaffinized in xylene for 5–10 min, followed by incubation in fresh xylene for another 5–10 min. The sections were then incubated in absolute ethanol for 5 min, 90% ethanol for 2 min, 70% ethanol for 2 min, and distilled water for 2 min. A proteinase K solution (20 μ g/mL, DNase-free, Beyotime, ST532) was added to the samples and incubated at 37 $^{\circ}$ C for 20 min. The sections were washed three times with PBS to remove residual proteinase K. The TUNEL detection solution was prepared using a TUNEL staining kit (Beyotime, C1089) at a 1:9 ratio of TdT enzyme to fluorescent labeling solution. A total of 50 μ L of TUNEL

detection solution was applied to each sample, followed by incubation at 37 °C in the dark for 60 min. The sections were then washed three times with PBS. Finally, the slides were mounted with anti-fluorescence quenching mounting medium and observed under a fluorescence microscope.

Bone marrow-derived macrophages (BMDM) isolation and culture

bone marrow cells from mice femur and tibia first underwent erythrocyte lysis, followed by seven days of culture in complete medium encompassing DMEM added with 10% heat-inactivated FBS and 30% L929-conditioned medium. To activate M1like, $(0.5-0.7) \times 10^6$ macrophages were arranged to receive 100 ng /mL LPS treatment (Invivogen) in tissue culture dishes.

RNA extraction and real-time PCR analysis

The QuantiTect Rev. Transcription Kit (Vazyme, Nanjing) was applied to synthesize the RNA obtained from cells or tissues (EASYspin Plus kit, Aidlab) to Complementary DNA (cDNA) and SYBR Green qPCR Mix served for the augmentation (Vazyme) on Bioer- Light-cycler. Table S1 in the Supporting Information lists the relevant primers and the Beijing Genomics Institute took charge of the corresponding synthesis.

Western blotting analysis

After three times of washed in cold PBS, macrophages underwent 30 min of lysis using protease and phosphatase inhibitor cocktails (selleck) by virtue of radioimmunoprecipitation assay (RIPA) (Beyotime). Quantification of protein concentration was based on the bicinchoninic acid (BCA) protein kit (Beyotime). After sodium dodecyl sulfate (SDS)-polyacrylamide gel electrophoresis, proteins samples were moved onto polyvinylidene fluoride or polyvinylidene difluoride (PVDF) membranes (Millipore), which received 1 h of blockage in 5% bovine serum albumin (BSA) (Solarbio) and 0.1% Tween 20 in Tris-buffered saline, followed by one night of incubation using primary antibody at 4 °C. Table S1 in the Supporting Information lists corresponding antibodies.

ELISA

We measured IL-1 β and IL-18 concentration in culture medium with an ELISA kit (#PI305, #PI558, Beyotime) as per producer's protocol, and used Sunrise spectrophotometer to examine the absorbance at 450 nm.

MeRIP-qPCR

we dissolved the total RNA (EASYspin Plus kit, Yishan, China) in RNase-free water (40 μ L). We assigned two groups of cells. One was for input and another (1 mL) receive 2 h of incubation with buffer (encompassing an

RNase inhibitor (RVC), an m6 A-specific antibody or rabbit IgG (Sigma Aldrich)), followed by another 2 h of incubation after added with prewashed beads, and 1 h of incubation at 4 °C after added with elution buffer that contained an anti-m6A antibody (Synaptic Systems). We used 5 mg of glycogen and 1/10 volumes of 3 M sodium acetate to precipitate the methylated mRNA in a 2.5 volume of 100% ethanol for one night at -80 °C. qPCR was employed for calculating the m6 A-bound RNA, which was normalized to the input to obtain relevant m6 A enrichment.

RNA stability assay

We used 5 μ g /mL actinomycin D to treat BMDMs seeded in 12-well plates and collected cells at specific time points (MedChemExpress), thereby measuring the stability of mRNA. RT-PCR was employed for analyzing the total RNA (EASY spin Plus kit, Aidlab). Linear regression analysis engaged in estimating the half-live time of mRNA.

RNA pull down assay

Biosune Biotechnology (Shanghai) took charge of the synthesis of single-stranded RNA that contained adenosine (regardless of methylation) (Table S1). Pierce RNA 3' End Desthiobiotinylation Kit and Pierce Magnetic RNA-Protein PullDown Kit (20163, 20164, Thermo Scientific) served for NLRP3 RNA desthiobiotin labeling and the RNA pulldown assays, respectively. In brief, 50 pmol of RNA underwent 5 min of denaturation at 85 °C and the T4 RNA ligase biotin labeling. After biotin labeling, nucleic acid underwent the incubation with streptavidin beads (50 μ L) coupled with BMDMs protein lysates (2 mg). At last, we boiled the eluted RNA-binding protein complexes meanwhile using anti-IGF2BP2 antibody for detection.

Cell culture and treatment

Culture conditions for ARPE-19 cells (Chi Scientific, Jiangsu, China) included: DMEM encompassing 10% FBS (Biological Industries, Italy). THP-1 cells (National Collection of Authenticated Cell Cultures) were cultured in RPMI 1640 (Gibco, USA) added with 10% FBS. THP-1 cells underwent one day of treatment using 100 μ M PMA for the formation of THP-1 macrophages (THP-M cells), seeded in a 6-well plate (1×10^6 cells/well). After coculture on inserts (diameter: 24 mm; pore diameter: 0.4 μ m; #3412, Corning, USA), RPE cells underwent 48 h of treatment using H₂O₂, (SML0583, Sigma-Aldrich, USA) followed by the co-culture with THP-1 cells. After 48 h of transfection with or without IGF2BP2 siRNA, THP-1 cells received 48 h of co-culture with RPE cells.

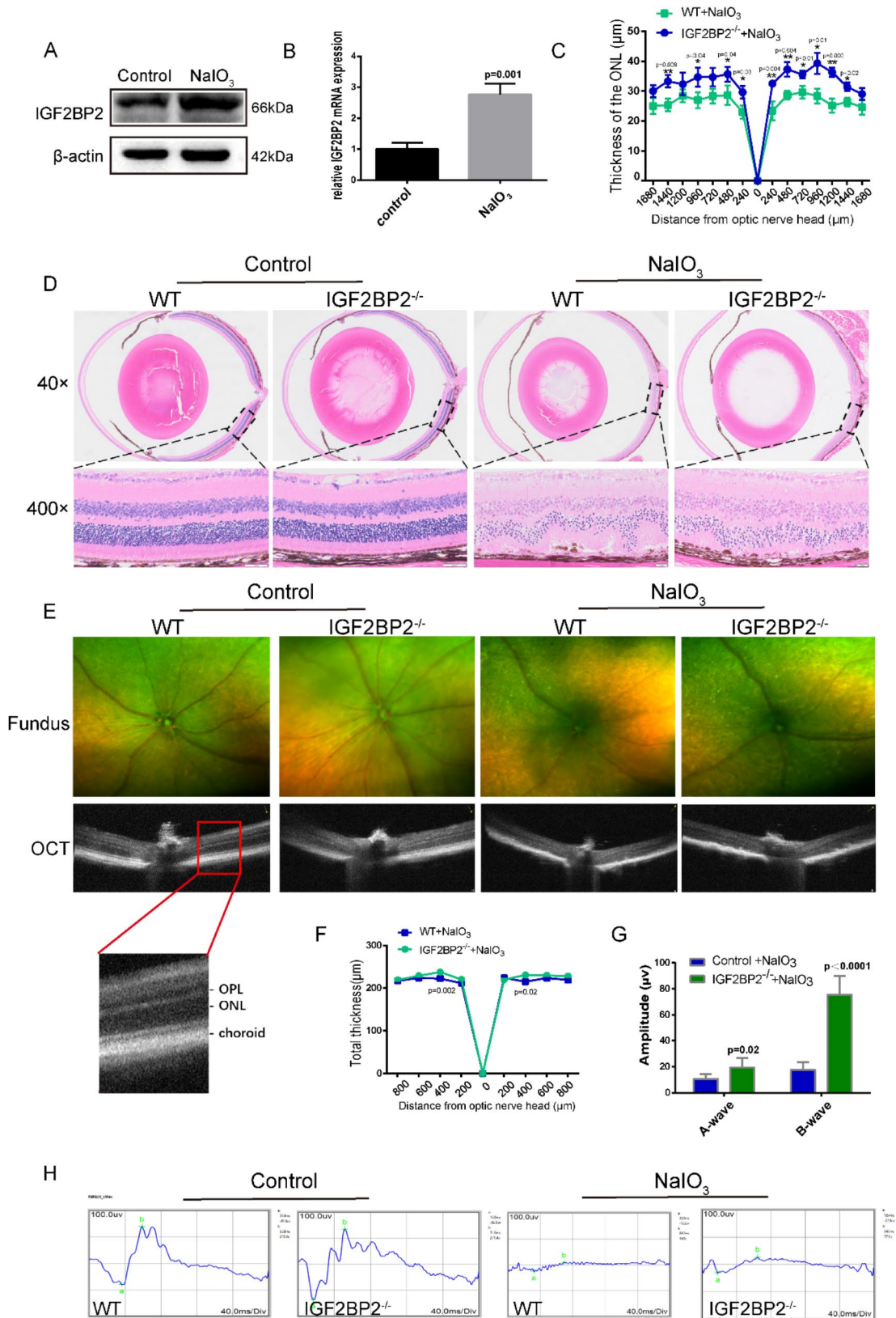


Fig. 1 (See legend on next page.)

(See figure on previous page.)

Fig. 1 IGF2BP2 participates in the disease progression of dry AMD **(A)** the expression of IGF2BP2 protein in retinal choroid tissue after NaIO₃ treatment. **(B)** The expression of IGF2BP2 mRNA in retinal choroid tissue after NaIO₃ treatment. $P=0.0016$ **(C)** Thickness of the ONL. **(D)** H&E staining revealed the histopathological changes in the retinas of WT and IGF2BP2^{-/-} mice, both in normal controls and 7 days after NaIO₃ administration. **(E-F)** Representative fundus images, SD-OCT images and a spider plot showing changes structure and thickness of fundus retina, keeping the optic nerve head (ONH) as the center position. **(G)** Amplitudes of the a- waves and b-waves. **(H)** Representative electroretinogram (ERG) of 24-hour dark adaptation mice. ONL outer nuclear layer; OPL outer plexiform layer. * $P < 0.05$, ** $P < 0.01$. Data are the means \pm SEM. Data are representative of results obtained from six mice in each group ($n=6$)

Transfection of siRNA

We used INTERFERin (Polplus) for transfecting cells with IGF2BP2 siRNAs, and Control siRNAs as per producer's protocol. 50 nmol siRNA together with 10 μ L of reagent were employed for transfecting BMDMs for 3 consecutive days, then experiments were conducted. Genepharma Company (Shanghai) took charge of the design and synthesis of targeting siRNA sequences (Table S1).

Flow cytometry

Cell Apoptosis Detection Kit (#556547, BD Bioscience, San Jose, CA, USA) served for detecting the cell apoptosis. Cells isolated by 0.25% trypsin were centrifugated at $300 \times g$ for five minutes, resuspended in the 1×10^6 cells/mL binding buffer, and cultured for fifteen minutes in Annexin V-FITC and propidium iodide reagents (1:20 dilution) in dark environment in succession. Cell analysis relied on an Accur C6 Plus cytometer (BD).

Hoechst staining assay (HSA)

Cells were properly treated, and received PBS wash after the removal of culture medium. After 10 min of fixation in 4% paraformaldehyde solution, cells with supernatant removed received another PBS wash. Subsequently, cells underwent 5 min of incubation in hoechst solution in dark environment at room temperature. An inverted fluorescence microscope (Olympus IX53, Japan) was employed to take 3 images for each well in a random manner.

Preparation of FA-MSN-CW11-2

The synthesis of MSN was carried out using a previously reported soft-template method to produce uniform MSN. The aminated mesoporous silica was then reacted overnight with excess NHS-PEG-FA (Ruixi Biological Technology Co., Ltd., Xian, China), followed by centrifugation and washing several times to obtain FA surface-modified mesoporous silica. Finally, FA surface-modified mesoporous silica was stirred overnight with CW11-2 and FITC at room temperature, and the resulting product, mesoporous silica nanoparticles loaded with CW11-2/FITC and surface-modified with FA, was collected by centrifugation and washing.

In vitro cellular uptake of NPs

For measuring the cellular uptake mode regarding NPs, experimenters loaded FITC into MSN, and seeded BMDM cells and RPE cells in six-well plates (2×10^5 cells/well) to undergo one day of culture. Cells received 2 h of treatment in FITC-loaded MSN medium, followed three times of washes in PBS and fixation treatment in paraformaldehyde. Cell absorption was measured using an Olympus BX53F fluorescence microscope.

Statistical analysis

GraphPad Prism 8.0 was employed for analyzing the between-group statistical difference. All data presentation followed the mean \pm SEM format. All experiments were repeated for no less than three times. The two-way ANOVA test served for comparing the mean value of a continuous variable regarding 2 samples. Unpaired Student's t-test served for the comparison regarding 2 groups. $P < 0.05$ indicated statistical significance.

Result

IGF2BP2 participates in the disease progression of dry AMD

In order to study the role of IGF2BP2 in dry AMD, we used the dry AMD model made by NaIO₃ (30 mg/kg) to examine the expression of IGF2BP2 in the retina and choroid complex of mice. We found that the mRNA and protein levels of IGF2BP2 were significantly increased in NaIO₃-mediated dry AMD mice (Fig. 1A-B). These results suggest that IGF2BP2 may be involved in regulating the progress of dry AMD. Next, we generated IGF2BP2-deficient (IGF2BP2^{-/-}) mice. In healthy control groups, no significant differences in retinal structure and function were observed between IGF2BP2^{-/-} and WT mice. However, in the dry AMD model, IGF2BP2^{-/-} mice exhibited a milder dry AMD phenotype compared to WT mice. H&E staining and OCT analysis showed that the retinal structure of IGF2BP2^{-/-} mice was less damaged and the outer nuclear layer was thicker (Fig. 1C-F). In addition, ERG analysis showed that the retinal function of IGF2BP2^{-/-} mice was better than that of WT mice (Fig. 1G-H). We found that IGF2BP2 deficiency alleviated the dry AMD phenotype of mice.

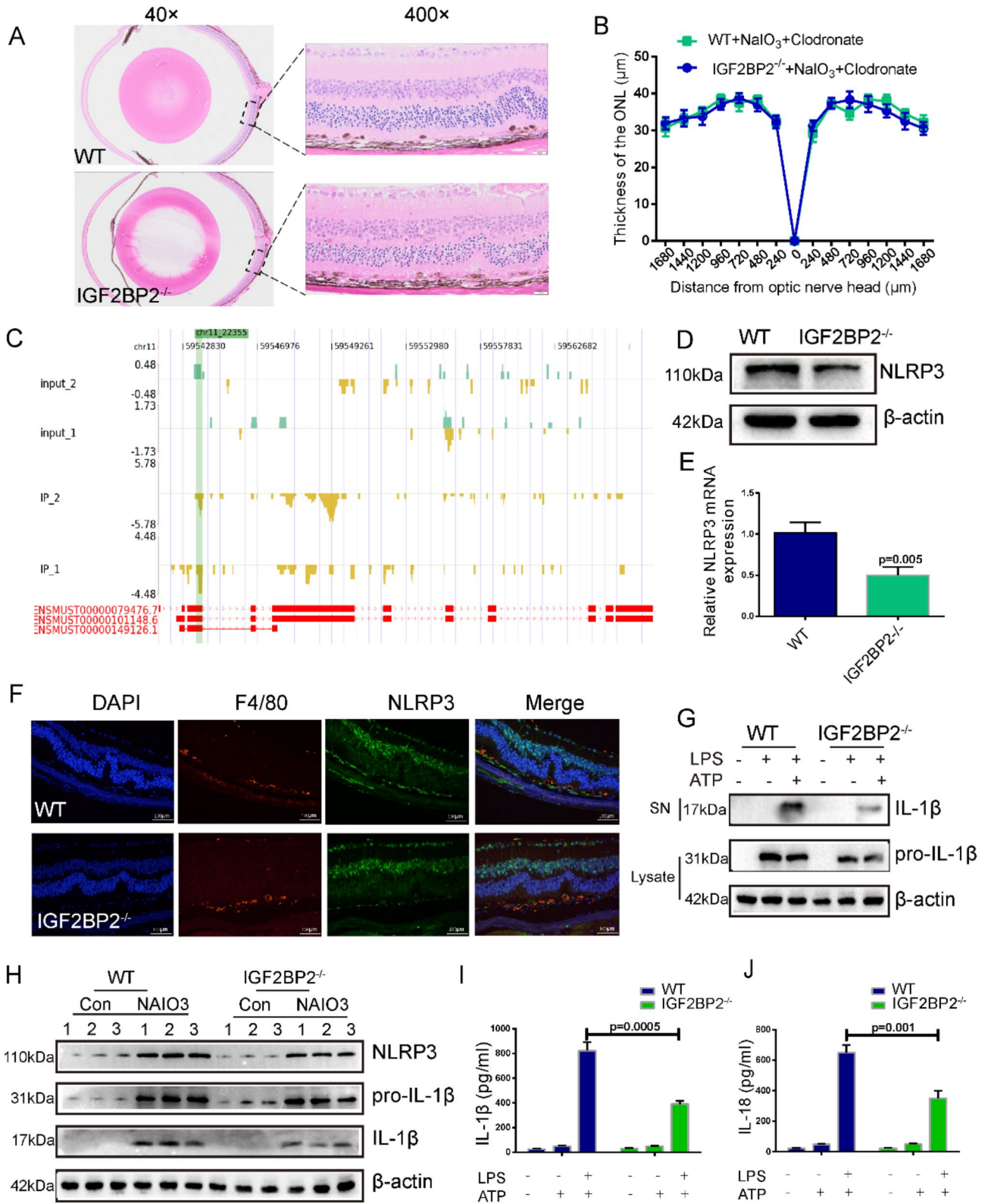


Fig. 2 (See legend on next page.)

(See figure on previous page.)

Fig. 2 IGF2BP2 affects activation of NLRP3 inflammatory bodies in macrophages **(A)** Representative H&E-stained retinal sections of WT and IGF2BP2^{-/-} groups after clodronate treatment. **(B)** Outer nuclear layer thickness in WT and IGF2BP2^{-/-} groups after clodronate treatment. **(C)** The reads density landscape of IGF2BP2-binding peaks on NLRP3 transcripts in BMDMs from IGF2BP2-iRIPseq; *n*=2. **(D)** the level of NLRP3 in BMDM stimulated by Lps was detected by western blot. **(E)** The expression of I NLRP3 mRNA in BMDM stimulated by Lps; *n*=3. **(F)** Expression of F4/80 (red) and NLRP3 (green) was observed in retinal tissue, cellular nuclei were labeled by DAPI (blue); Scale bars: 50 μm. **(G)** BMDMs from IGF2BP2 knockout mice and wild mice was initiated with LPS and stimulated with ATP. The supernatant (SN) and cell extract (lysate) were analyzed by immunoblotting. **(H)** the retina and choroid tissue extracts of IGF2BP2 knockout mice and wild mice were analyzed by Western blotting. **(I-J)** IL-1β and IL-18 secretion was determined by ELISA. ** *p* < 0.01, *** *p* < 0.001. The data is the average ± SEM

IGF2BP2 affects activation of NLRP3 inflammatory bodies in macrophages

To investigate whether the retinal damage observed in IGF2BP2^{-/-} mice was caused by the inflammatory recruitment of macrophages [22, 24], we assessed the effects of clodronate, a chemical agent that induces macrophage apoptosis and subsequently leads to macrophage depletion [25]. Histological analysis showed that, compared to the NaIO₃-injected group, macrophage depletion using clodronate liposomes before NaIO₃ injection prevented NaIO₃-induced thinning of the ONL. However, after macrophage depletion, the difference in ONL thickness between IGF2BP2^{-/-} mice and WT mice disappeared (Fig. 2A-B). These data suggest that IGF2BP2-deficient macrophages play a key role in and mitigate NaIO₃-induced retinal damage in mice. Regarding the targets of IGF2BP2 in macrophages, our analysis of previous data revealed that iRIP identified NLRP3 was one of the mRNAs associated with IGF2BP2 in two separate replicates [22] (Fig. 2C). we also find the expression of NLRP3 in IGF2BP2^{-/-}BMDM was down-regulated compared with WT (Fig. 2D-E). Meanwhile, in the NaIO₃-induced dry AMD model, we noticed that compared to the WT group, the immunofluorescence staining of NLRP3 was reduced in IGF2BP2^{-/-} mice and co-localized with macrophages (Fig. 2F), and the retinal choroidal complex NLRP3 expression decreased in IGF2BP2^{-/-} mice (Fig. 2H). In order to study whether IGF2BP2 in macrophages contributes to the activation of NLRP3 inflammatory bodies, we treated BMDM induced by lipopolysaccharide with agonists. BMDM from IGF2BP2^{-/-} mice showed impaired activation of NLRP3 inflammatory bodies triggered by ATP, which inhibited the maturation and secretion of IL-1β (Fig. 2G, I, J). In conclusion, these results suggest that IGF2BP2 supports NaIO₃-induced dry AMD by promoting the expression of NLRP3 in macrophages and the activation of inflammatory body-dependent IL-1β.

IGF2BP2 targets NLRP3 in an m6A-dependent manner, contributing to the apoptosis of RPE cells

Given the characteristic role of IGF2BP2 as an mRNA-binding protein, we ultimately aimed to investigate whether IGF2BP2 directly interacts with NLRP3. We detected the M6A level of NLRP3 in BMDM by MERIP-qPCR, and the results showed that M6A modified

the expression of NLRP3 (Fig. 3A). By analyzing iRIP sequencing data and corresponding peaks, we designed single-stranded RNA baits with methylation (ss-m6A) and unmethylated controls (ss-A) for RNA pull-down assays. The RNA pull-down assay, in agreement with the MeRIP-qPCR results, demonstrated that IGF2BP2 protein selectively binds to the methylated RNA bait (ss-m6A) of NLRP3 (Fig. 3B). RNA decay assessment reports that NLRP3mRNA with IGF2BP2 defects decays faster than WT BMDM (Fig. 3C-D), indicating that IGF2BP2 can improve the stability of NLRP3mRNA. In summary, these data suggest that IGF2BP2 regulates the expression of NLRP3 in macrophages in an M6A-dependent manner. One of the key mechanisms of dry AMD progression is RPE dysfunction and loss of apoptosis, Evidence indicates that macrophages exhibiting inflammatory activity can inflict varying degrees of damage on RPE cells, from sublethal to lethal [26]. To investigate the effect of IGF2BP2 in inflammatory macrophages on RPE cell apoptosis, we used ARPE-19 (human RPE cell) and co-cultured them with PMA-induced THP-1 (human macrophage cell). First, we knocked down IGF2BP2 in THP-1 macrophages using siRNA and verified the knockdown efficiency (Figs. 3E-F). Next, THP-1 cells were incubated with RPE cells after PMA, LPS and ATP treatment for 24 h (Fig. 3G), and RPE cells were collected to detect apoptosis. Nuclear morphological changes were examined using Hoechst staining. In the normal control group, apoptotic cells were rarely observed. However, after co-culturing with macrophages (MP), condensed RPE cell nuclei and enhanced fluorescence (yellow arrows) were observed, indicating an increase in the number of apoptotic RPE cells compared to the normal control group. In contrast, in the MP + SiIGF2BP2 group, a significant reduction in RPE cell apoptosis was observed compared to the MP co-culture group. (Fig. 3H). Secondly, the number of apoptotic cells was significantly higher in the MP co-culture group compared to the normal control group. In contrast, The MP + SiIGF2BP2 group showed a significant decrease in apoptotic cell numbers compared to the MP co-culture group (Fig. 3I). These results suggest that macrophages can affect the apoptosis of RPE through IGF2BP2.

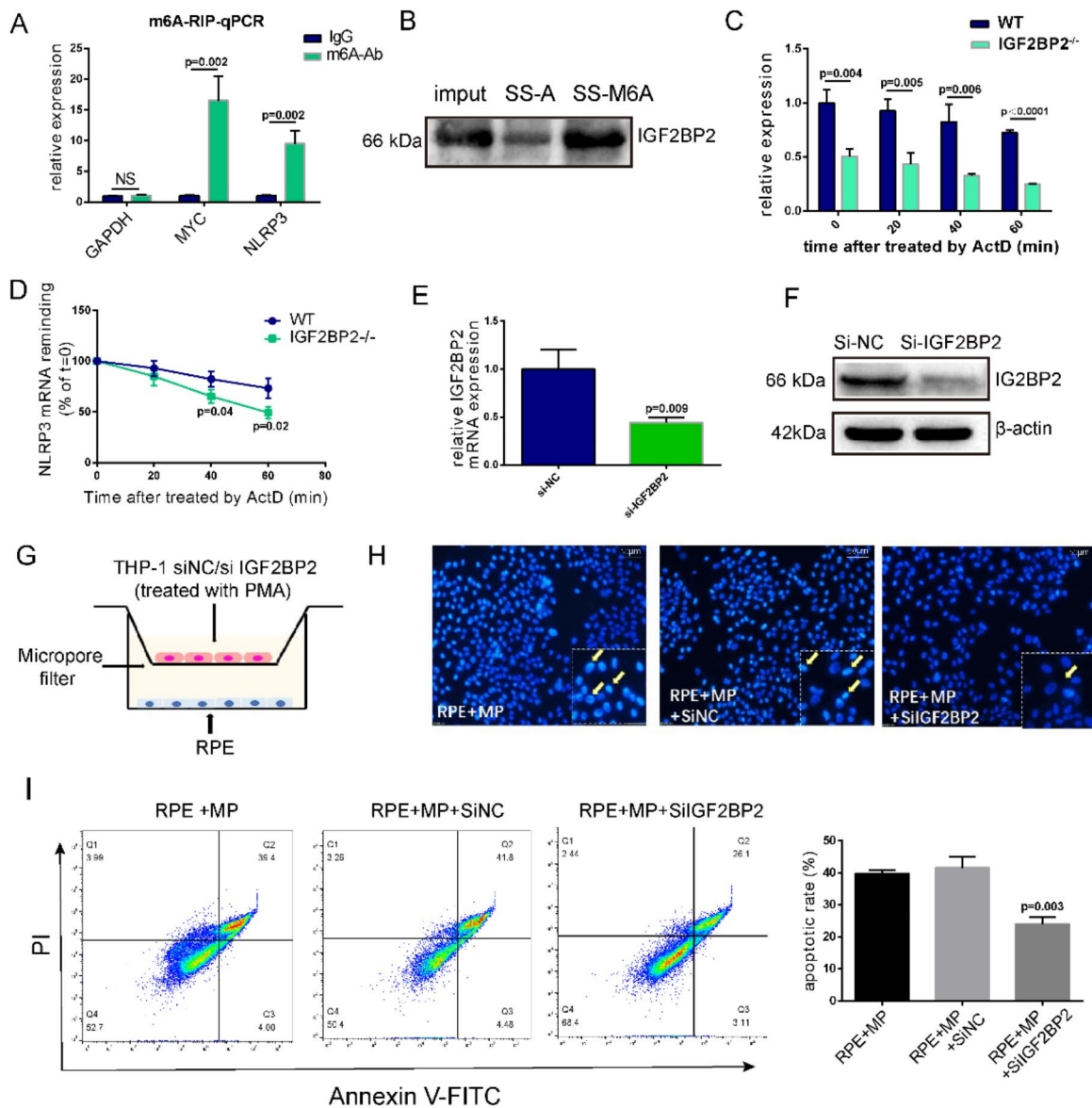


Fig. 3 Macrophage IGF2BP2 targets NLRP3 in an m6A-dependent manner, contributing to the apoptosis of RPE cells. **(A)** m6A enrichment of NLRP3 mRNA in BMDMs by m6A-RIP-qPCR. Results are presented relative to those obtained with immunoglobulin G (IgG). Glyceraldehyde 3-phosphate dehydrogenase (Gapdh), m6A negative control; Myc peak, m6A positive control; $n=3$. **(B)** Immunoblotting of IGF2BP2 in BMDMs after RNA pull down assay using single-stranded NLRP3 RNA with methylated or unmethylated adenosine. **(C-D)** RT-qPCR of **(C)** NLRP3 mRNAs and **(D)** NLRP3 mRNA degradation in BMDMs treated with actinomycin D for the indicated times. The residual RNAs were normalized to 0 h; $n=5$. **(E-F)** PCR and Western blot analysis of IGF2BP2 in THP-1 following si-NC or si-IGF2BP2 transfection to verify the knockdown effect. **(G)** Co-culture model of RPE and macrophages. **(H)** Analysis of nuclear morphological changes in ARPE-19 cells using Hoechst staining, with yellow arrows indicating damaged cells. **(I)** Detection of apoptosis in ARPE-19 cells using Annexin V-FITC/PI double staining and flow cytometry. Data were shown as mean \pm SEM. * $P<0.05$; ** $p<0.01$, *** $p<0.001$, **** $p<0.0001$ versus the WT group by two-way ANOVA

Synthetic identification and safety of FA-MSN-CWI1-2

Our previous study demonstrated that targeting macrophages with nanoparticles yielded promising therapeutic effects in AMD [27]. In this study, MSN loaded with CWI1-2 was first prepared, followed by surface conjugation with FA on the NPs. Since activated M1 macrophages express Folate Receptor 2 (FR2), MSN-CWI1-2 was modified with FA to achieve active targeting of M1

macrophages [28]. The average particle size of FA-MSN-CWI1-2 was 133.613 ± 1.62 nm, with a zeta potential of -10.457 ± 0.79 mV. The polydispersity index (PDI) value was 0.186 ± 0.03 , indicating stability and good dispersibility (Table 1). The morphology and size of the NPs were characterized by TEM, which revealed a spherical structure, in addition, the UV absorption peak of the nanomaterials was measured (Fig. 4B-C). Regarding

Table 1 Particle size and potential

	Hydrodynamic size (nm)	PDI	Zeta potential (mV)
1	133.92	0.217	-10.29
2	131.86	0.182	-9.76
3	135.06	0.159	-11.32
Average	133.613±1.62	0.186±0.03	-10.457±0.79

cellular delivery using nanomaterials, FA-MSN-CWI1-2 demonstrated significantly higher binding affinity to macrophages compared to RPE cells. Additionally, in frozen sections of ocular tissue, FITC fluorescence was clearly observed accumulating within the retina, indicating its strong tissue targeting and penetration capabilities (Fig. 4D). To assess the safety of the drug, OCT and fundus photography were performed on healthy mice at days 1, 3, and 7 after intravitreal injection, and no significant retinal structural changes were observed in the FA-MSN-CWI1-2 group compared to the control group (Fig. 4E). Moreover, TUNEL⁺ cell counting and histological analysis showed no evidence of significant toxicity in the retina following various treatments, indicating that the drug is safe (Fig. 4F).

FA-MSN-CWI1-2 as a strategy against dry AMD

we evaluated the role of FA-MSN-CWI1-2 in the NaIO₃-induced mouse model, administering FA-MSN-CWI1-2 (5.0 mg/mL dispersed in DPBS) via intravitreal injection on days 1 and 3. Mice receiving intravitreal injections of DPBS were used as a negative control. qPCR results

confirmed that the relative IGF2BP2 levels in the retinas of dry AMD mice treated with FA-MSN-CWI1-2 were significantly reduced 7 days post-treatment compared to control mice (Fig. 5A), indicating effective *in vivo* delivery by CWI1-2. Subsequently, retinal structure and ONL thickness changes were analyzed using HE staining and OCT. The ONL thickness in FA-MSN-CWI1-2 treated mice were significantly greater than that in the control group treated with DPBS (Fig. 5B-C). Furthermore, ERG analysis combined with TUNEL + cell counting indicated an improvement in retinal function in the FA-MSN-CWI1-2 treatment group compared to the control group (Fig. 5D-E, G-H). To characterize changes in the retinal immune microenvironment following FA-MSN-CWI1-2 treatment, we further assessed the expression of the NLRP3 inflammasome in retinal-choroidal tissue using WB (Fig. 5F). Compared to the control group, FA-MSN-CWI1-2 treatment reduced the expression of the NLRP3 inflammasome in the retinal-choroidal complex. These data provide strong evidence that IGF2BP2 can indeed exert its effects through macrophages.

Discussion

This study found that IGF2BP2 levels were increased in the retina and choroid tissues of NaIO₃-induced dry AMD mice. IGF2BP2 enhances the stability of NLRP3 mRNA in macrophages in an m6A-dependent manner, thereby participating in disease progression. Meanwhile, we established the FA-MSN-CWI1-2 delivery system,

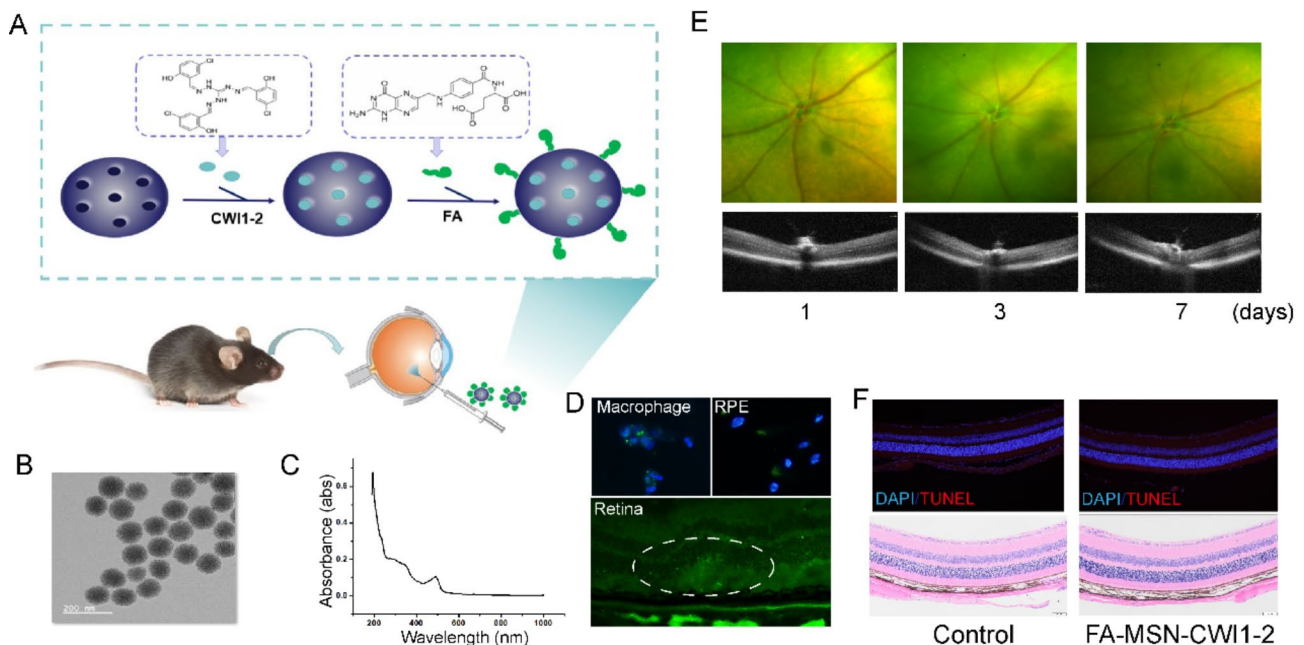


Fig. 4 Synthetic identification and safety of FA-MSN-CWI1-2 (A) Schematic diagram shows the synthesis of folic acid-modified mesoporous silica nanoparticles loaded with CWI1-2 (FA-MSN-CWI1-2). (B) TEM image and particle size distribution of FA-MSN-CWI1-2. (C) UV-vis of FA-MSN-CWI1-2. (D) FA-MSN-CWI1-2 was co-cultured with cells for 2 h, and 7 days after intravitreal injection, FITC fluorescence was observed. (E) Retinal photography and OCT images of healthy mice 1, 3, and 7 days after intraocular injection. (F) HE and TUNEL histological staining of representative retinal tissue in different groups

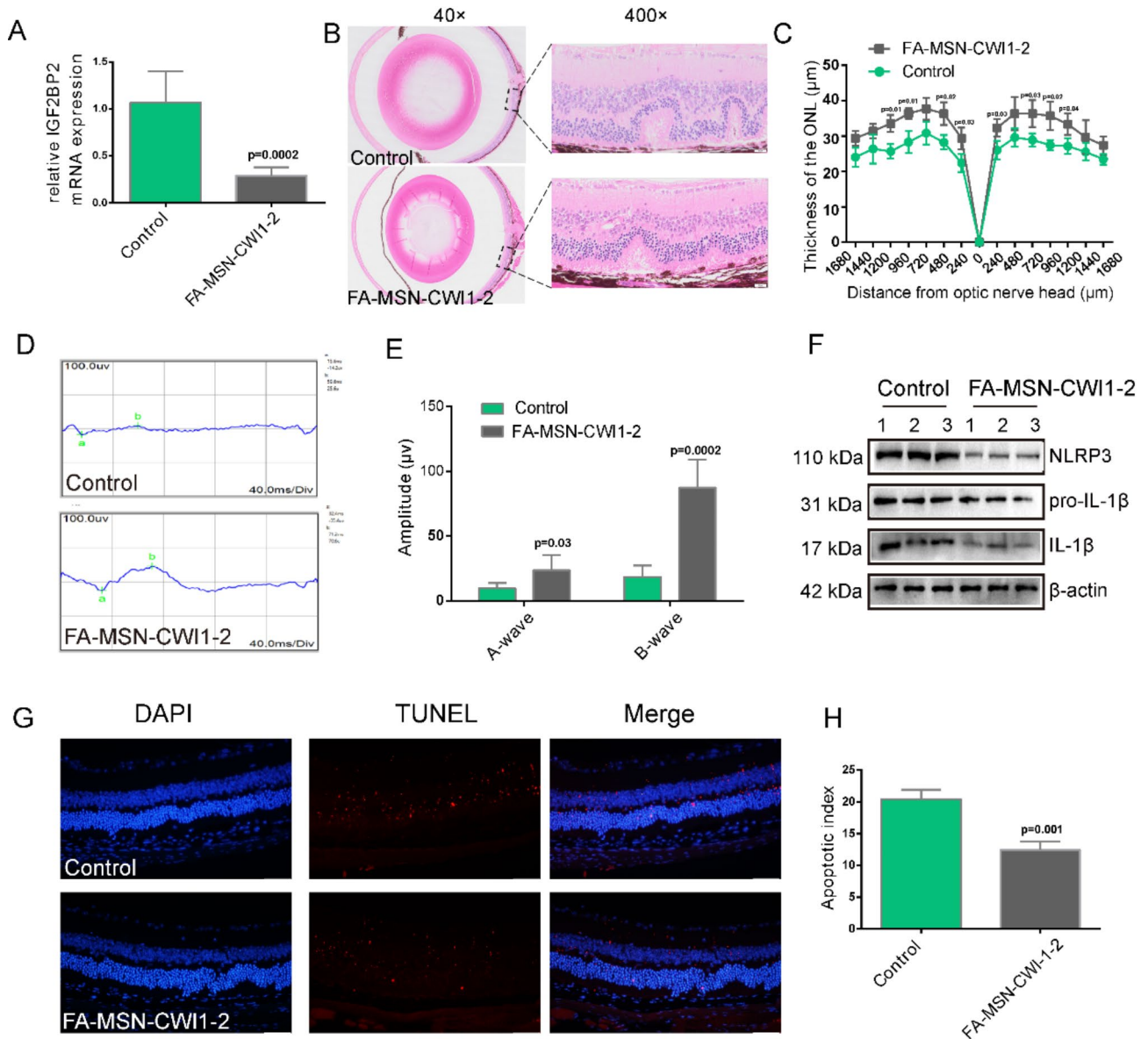


Fig. 5 FA-MSN-CWI1-2 as a strategy against dry AMD. **(A)** The expression of IGF2BP2 mRNA in retinal choroid tissue after NaIO₃ treatment. **(B)** Histopathological changes of retina were analyzed by H & E staining. **(C)** The spider diagram shows the change in the thickness of the ONL layer of the retina, keeping the ONH at the center. **(D)** Representative electroretinogram (ERG) of 24-hour dark adaptation mice. **(E)** Amplitudes of the a-waves and b-waves. **(F)** the retina and choroid tissue extracts were analyzed by Western blotting. **(G)** Representative TUNEL staining of retinal tissues from different groups. **(H)** Analysis of apoptotic index. * *P* < 0.05, ** *P* < 0.01. Data are the means ± SEM. Data are representative of results obtained from six mice in each group (*n* = 6)

which further provides evidence for the involvement of macrophage IGF2BP2 in the progression of dry AMD (Fig. 6).

Initially, we highlighted the characteristics and potential functions of IGF2BP2 in dry AMD. Currently, numerous investigations are underway to explore the function and mechanisms of m6A modification in dry AMD. m6A modification mediated by YTHDC1 has been shown to protect against oxidative stress damage and maintain lipid metabolism in RPE cells in dry AMD by regulating the expression of CircSPECC1 [29]. In Aβ-induced RPE

degeneration, FTO-dependent m6A demethylation of protein kinase A regulates its mRNA and protein expression, partially rescuing RPE degeneration [30]. These findings suggest that targeted modulation of IGF2BP2-mediated m6A modification may represent a breakthrough in the management of dry AMD. Nevertheless, the precise role of m6A modification in dry AMD, especially its detailed mechanisms, remains largely unknown and warrants further investigation. In this research, we identified significantly elevated levels of IGF2BP2 expression in the NaIO₃-induced dry AMD mouse model.

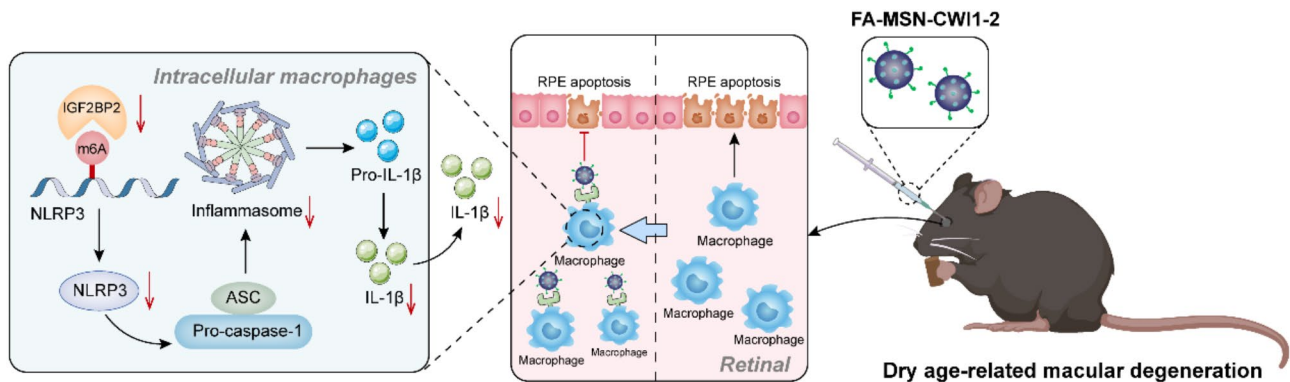


Fig. 6 Mechanistic Insights into IGF2BP2's Role in Macrophage-Mediated Pathogenesis of Dry AMD

Moreover, IGF2BP2 knockout notably alleviated retinal structural and functional damage, indicating a positive correlation between elevated IGF2BP2 levels and the progression of dry AMD. Hence, modulation of IGF2BP2 may offer a novel strategy for the treatment of dry AMD.

Inflammation and immune-mediated processes play a crucial role in the progression of AMD [31]. Macrophage infiltration is both a consequence of tissue injury and a result of dysregulated immune suppression mechanisms that are supposed to limit macrophage entry into the subretinal space. Consistent with previous studies, our findings indicate that macrophage depletion inhibits NaIO₃-induced ONL thinning. Meanwhile, we observed that the difference in ONL thickness between IGF2BP2^{-/-} mice and WT mice lost statistical significance. These findings suggest that macrophages are closely associated with the progression of dry AMD in the NaIO₃-induced model, with IGF2BP2 playing a key role primarily in macrophages.

Macrophages are highly plastic cells whose phenotype and function depend on their microenvironment [32]. Inflammatory conditions favor the polarization of M1 macrophages, which produce high levels of pro-inflammatory cytokines such as IL-1β, TNF-α, IL-6, and IL-12, as well as inducible nitric oxide synthase (iNOS), leading to a Th1-type immune response [33, 34]. Classically activated M1 macrophages are stimulated by lipopolysaccharide (LPS) and interferon-gamma (IFN-γ). LPS, a component of the Gram-negative bacterial cell wall, binds to macrophages via the TLR4 receptor, activating signaling pathways such as NF-κB and MAPK, thereby inducing pro-inflammatory responses and M1 polarization. Conversely, Th2-type cytokines IL-4 and IL-13 serve as direct activators of M2 macrophages [31]. These cytokines are secreted by various cell types, including innate and adaptive immune cells, epithelial cells, and tumor cells. In addition to playing crucial roles in physiological processes such as homeostasis, wound healing, and tissue repair, M2 macrophages are also involved in pathological conditions, including inflammation, hypersensitivity

reactions, and choroidal neovascularization [35, 36]. Interestingly, regarding the role of IGF2BP2 in macrophages, Wang et al. found that IGF2BP2-deficient macrophages exhibited an enhanced M1 phenotype, which promoted the development of dextran sulfate sodium (DSS)-induced colitis [22]. Unlike previous studies, which focused on macrophage polarization, our study primarily investigates the regulatory effects of macrophages on the NLRP3 inflammasome in the context of dry AMD, where the inflammatory role of M1 macrophages is a key factor. Macrophages exhibit substantial heterogeneity across different tissues, performing tissue-specific functions [37, 38]. They are distinguished based on microenvironmental cues, leading to diverse gene expression profiles and functional characteristics [39, 40]. Thus, IGF2BP2 may exert distinct effects on macrophages depending on tissue type and specific challenges. The classification of macrophage subtypes is not limited to the M1 and M2 paradigm; instead, macrophage polarization is a dynamic and complex process. Although M1 and M2 are the most widely discussed phenotypes, macrophages can exhibit a spectrum of activation states in response to different stimuli, with overlapping characteristics rather than strictly independent classifications. In dry AMD, single-cell RNA sequencing of blood-derived macrophages has been employed to elucidate their roles in disease progression [41, 42]. Future studies are expected to further characterize specific macrophage subtypes and their functional properties, which will contribute to a more comprehensive understanding of the potential role of IGF2BP2 in regulating macrophage function.

Infiltrating macrophages may contribute to the pathobiology of AMD by activating the NLRP3 inflammasome and other pro-inflammatory cytokines [43, 44]. Following PAMP or DAMP stimulation, IL-1β is initially produced in an immature form within macrophages. IL-1β can then trigger the assembly of the NLRP3 inflammasome in macrophages, activating caspase-1, which cleaves pro-IL-1β into its mature form. This active cytokine is secreted and further amplifies the production of inflammatory

cytokines through positive feedback [45, 46]. Previous studies have shown that certain components of the lupus-associated autoantigen and complement protein C1q can activate the NLRP3 inflammasome in macrophages, promoting IL-1 β secretion [47, 48]. Age-related lipofuscin can similarly activate the NLRP3 inflammasome. Once activated, IL-1 β signaling amplifies inflammation in the rodent eye by inducing the expression of chemokines such as CCL2, CXCL1, and CXCL10 [49, 50]. To support the role of IGF2BP2 in regulating retinal injury through the activation of the macrophage NLRP3 inflammasome, we observed that the expression of inflammasome component NLRP3 was reduced in the retinas of IGF2BP2^{-/-} mice and was colocalized with infiltrating subretinal macrophages (F4/80⁺). We also validated our findings in retinal-choroidal tissue and bone marrow-derived primary macrophages.

Regarding the source of NLRP3 inflammasome-expressing cells in the eye in dry AMD, there has been debate about the presence of NLRP3 in RPE cells. However, consistent with our study, recent research on the expression of NLRP3 in single-cell RPE tissue indicates that NLRP3 levels are lower in RPE cells compared to macrophages, reinforcing our focus on macrophages [51, 52]. Given the critical role of NLRP3 inflammasome activation in infiltrating macrophages for the production of IL-1 β [14], and increasing evidence from retinal mouse models showing that enhanced macrophage infiltration into the subretinal space mediates RPE cell damage and photoreceptor death through direct cell interactions and paracrine release of inflammatory cytokines, we intentionally devised an experiment to demonstrate that activated BMDMs, known to produce high levels of IL-1 β , can induce RPE cell apoptosis, which can be mitigated by IGF2BP2 knockout.

In the posterior segment of the eye, circulating immune cells are generally prevented from accessing the retina. This is attributed to the tight junctions within the RPE that form the outer retinal blood barrier, along with the endothelial cells that create the inner retinal barrier. However, following injury, inflammation, or infection, circulating immune cells can migrate into the retina and preretinal membranes [53]. In this study, we employed a nanomaterial-based IGF2BP2 inhibitor delivery platform (FA-MSN-CWI1-2). The primary advantage of this platform is its ability to specifically target activated macrophages within the eye while safeguarding other retinal tissues from damage. Moreover, unlike macrophage-specific conditional knockout mice, this approach does not affect the systemic expression of macrophages in mice, thus allowing for a more precise elucidation of previous *in vitro* findings. We found that intravitreal injection of FA-MSN-CWI1-2 nanoparticles significantly reduced retinal damage caused by sodium iodate and also reduced

NLRP3 inflammasome levels. These results suggest that IGF2BP2 contributes to the progression of dry AMD, at least in part, through macrophages. However, whether other cell types are involved remains to be explored in future experiments.

Conclusion

In summary, this research provides strong *in vitro* and evidence highlighting the pivotal role of IGF2BP2 in regulating NLRP3 inflammasome activation in macrophages associated with dry AMD. The potential of Igf2bp2 in macrophages as a therapeutic target for dry AMD offers a promising direction for future research in the treatment of this disease.

Supplementary Information

The online version contains supplementary material available at <https://doi.org/10.1186/s13062-025-00648-5>.

Supplementary Material 1

Supplementary Material 2

Author contributions

YuQing Zhao, Yi Qu designed the research; YuQing Zhao, Yu Zhang, Junfang Li performed the experiments and analysed the data; YuQing Zhao, Yifei Zhang drafted the manuscript; Yi Qu revised.

Funding

This work was supported by Qilu Hospital of Shandong University.

Data availability

No datasets were generated or analysed during the current study.

Declarations

Competing interests

The authors declare no competing interests.

Received: 29 January 2025 / Accepted: 5 April 2025

Published online: 22 April 2025

References

1. Fleckenstein M, et al. Age-related macular degeneration. *Nat Rev Dis Primers*. 2021;7(1):31.
2. de Cabral TA, et al. Treatments for dry age-related macular degeneration: therapeutic avenues, clinical trials and future directions. *Br J Ophthalmol*. 2022;106(3):297–304.
3. Guymier RH, Campbell TG. Age-related macular degeneration. *Lancet*. 2023;401(10386):1459–72.
4. Waseem M, Al-Zamil, Sanaa A, Yassin. Recent developments in age-related macular degeneration: a review. *Clin Interv Aging*; 2017.
5. Geetika K, Nikhlesh K, Singh. Inflammation and retinal degenerative diseases. *Neural Regen Res*; 2022.
6. McLeod DS, et al. Distribution and quantification of choroidal macrophages in human eyes with Age-Related macular degeneration. *Invest Ophthalmol Vis Sci*. 2016;57(14):5843–55.
7. Lad EM, et al. Abundance of infiltrating CD163+ cells in the retina of post-mortem eyes with dry and neovascular age-related macular degeneration. *Graefes Arch Clin Exp Ophthalmol*. 2015;253(11):1941–5.

8. Krause TA, et al. VEGF-production by CCR2-dependent macrophages contributes to laser-induced choroidal neovascularization. *PLoS ONE*. 2014;9(4):e94313.
9. Mettu PS, et al. Retinal pigment epithelium response to oxidant injury in the pathogenesis of early age-related macular degeneration. *Mol Aspects Med*. 2012;33(4):376–98.
10. Krogh Nielsen M, et al. Patients with a fast progression profile in geographic atrophy have increased CD200 expression on Circulating monocytes. *Clin Exp Ophthalmol*. 2019;47(1):69–78.
11. Simi A, et al. Interleukin-1 and inflammatory neurodegeneration. *Biochem Soc Trans*. 2007;35(Pt 5):1122–6.
12. Allingham MJ, et al. Immunological aspects of Age-Related macular degeneration. *Adv Exp Med Biol*. 2021;1256:143–89.
13. Calkova L, Doyle SL, Campbell M. NLRP3 inflammasome and pathobiology in AMD. *J Clin Med*. 2015;4(1):172–92.
14. Dabouz R, et al. An allosteric interleukin-1 receptor modulator mitigates inflammation and photoreceptor toxicity in a model of retinal degeneration. *J Neuroinflammation*. 2020;17(1):359.
15. Zhao BS, Roundtree IA, He C. Post-transcriptional gene regulation by mRNA modifications. *Nat Rev Mol Cell Biol*. 2017;18(1):31–42.
16. Liu J, et al. A METTL3-METTL14 complex mediates mammalian nuclear RNA N6-adenosine methylation. *Nat Chem Biol*. 2014;10(2):93–5.
17. Ping XL, et al. Mammalian WTAP is a regulatory subunit of the RNA N6-methyladenosine methyltransferase. *Cell Res*. 2014;24(2):177–89.
18. Zhou H, et al. Extracellular vesicles derived from human umbilical cord mesenchymal stem cells alleviate osteoarthritis of the knee in mice model by interacting with METTL3 to reduce m6A of NLRP3 in macrophage. *Stem Cell Res Ther*. 2022;13(1):322.
19. Hao WY, et al. RNA m6A reader YTHDF1 facilitates inflammation via enhancing NLRP3 translation. *Biochem Biophys Res Commun*. 2022;616:76–81.
20. Cao J, et al. Insulin-like growth factor 2 mRNA-Binding protein 2-a potential link between type 2 diabetes mellitus and cancer. *J Clin Endocrinol Metab*. 2021;106(10):2807–18.
21. Dai N. The diverse functions of IMP2/IGF2BP2 in metabolism. *Trends Endocrinol Metab*. 2020;31(9):670–9.
22. Wang X, et al. The m6A reader IGF2BP2 regulates macrophage phenotypic activation and inflammatory diseases by stabilizing TSC1 and PPAR γ . *Adv Sci (Weinh)*. 2021;8(13):2100209.
23. Li M et al. Small molecule SIRT1 activators counteract oxidative stress-induced inflammasome activation and nucleolar stress in retinal degeneration. *Int Immunopharmacol*. 2024;142(Pt B):113167.
24. Olivier L, et al. Apolipoprotein E promotes subretinal mononuclear phagocyte survival and chronic inflammation in age-related macular degeneration. *EMBO Mol Med*; 2015.
25. Naito M et al. Liposome-encapsulated dichloromethylene diphosphonate induces macrophage apoptosis in vivo and in vitro. *J Leukoc Biol*, 1996.
26. Somasundaran S, et al. Retinal pigment epithelium and age-related macular degeneration: A review of major disease mechanisms. *Clin Exp Ophthalmol*. 2020;48(8):1043–56.
27. Zhang Y, et al. M2-type macrophage-targeted delivery of IKK β siRNA induces M2-to-M1 repolarization for CNV gene therapy. *Nanomedicine*. 2024;57:102740.
28. Tie Y, et al. Targeting folate receptor B positive tumor-associated macrophages in lung cancer with a folate-modified liposomal complex. *Signal Transduct Target Ther*. 2020;5(1):6.
29. Xue C et al. m(6)A modification of circSPECC1 suppresses RPE oxidative damage and maintains retinal homeostasis. *Cell Rep*, 2022.
30. Hu Y, et al. Fat mass and obesity-associated protein alleviates A β (1–40) induced retinal pigment epithelial cells degeneration via PKA/CREB signaling pathway. *Cell Biol Int*. 2023;47(3):584–97.
31. Kauppinen A, et al. Inflammation and its role in age-related macular degeneration. *Cell Mol Life Sci*. 2016;73(9):1765–86.
32. David M, Mosser, Justin P, Edwards. Exploring the full spectrum of macrophage activation. *Nat Rev Immunol*, 2008.
33. David M, Mosser. The many faces of macrophage activation. *J Leukoc Biol*, 2003.
34. María F-V, Silvia, González-Ramos, and Lisardo, Boscá. Involvement of monocytes/macrophages as key factors in the development and progression of cardiovascular diseases. *Biochem J*, 2014.
35. Hui Z et al. Age-dependent changes in FasL (CD95L) modulate macrophage function in a model of age-related macular degeneration. *Invest Ophthalmol Vis Sci*.
36. Siamon G, Fernando O, Martinez. Alternative activation of macrophages: mechanism and functions. *Immunity*, 2010.
37. Fernando C-G et al. T cells and macrophages responding to oxidative damage cooperate in pathogenesis of a mouse model of age-related macular degeneration. *PLoS ONE*, 2014.
38. Małgorzata N et al. Age-related macular degeneration in the aspect of chronic low-grade inflammation (pathophysiological parainflammation). *Mediators Inflamm*, 2014.
39. Siamon G, Annette P. Tissue macrophages: heterogeneity and functions. *BMC Biol*, 2017. 15(1).
40. Italiani P, Boraschi D. From monocytes to M1/M2 macrophages: phenotypical vs. Functional differentiation. *Front Immunol*. 2014;5:514.
41. Voigt AP, et al. Choroidal endothelial and macrophage gene expression in atrophic and neovascular macular degeneration. *Hum Mol Genet*. 2022;31(14):2406–23.
42. Droho S, et al. Ocular macrophage origin and heterogeneity during steady state and experimental choroidal neovascularization. *J Neuroinflammation*. 2020;17(1):341.
43. Brandli A, Vessey KA, Fletcher EL. The contribution of pattern recognition receptor signalling in the development of age related macular degeneration: the role of toll-like-receptors and the NLRP3-inflammasome. *J Neuroinflammation*. 2024;21(1):64.
44. Tseng WA, et al. NLRP3 inflammasome activation in retinal pigment epithelial cells by lysosomal destabilization: implications for age-related macular degeneration. *Invest Ophthalmol Vis Sci*. 2013;54(1):110–20.
45. Allan SM, Tyrrell PJ, Rothwell NJ. Interleukin-1 and neuronal injury. *Nat Rev Immunol*. 2005;5(8):629–40.
46. Schroder K, Tschopp J. The inflammasomes. *Cell*. 2010;140(6):821–32.
47. Doyle SL, et al. NLRP3 has a protective role in age-related macular degeneration through the induction of IL-18 by Drusen components. *Nat Med*. 2012;18(5):791–8.
48. Gao J, et al. Evidence for the activation of pyroptotic and apoptotic pathways in RPE cells associated with NLRP3 inflammasome in the rodent eye. *J Neuroinflammation*. 2018;15(1):15.
49. Natoli R, et al. Microglia-derived IL-1 β promotes chemokine expression by Müller cells and RPE in focal retinal degeneration. *Mol Neurodegener*. 2017;12(1):31.
50. Brandstetter C, et al. Inflammasome priming increases retinal pigment epithelial cell susceptibility to Lipofuscin phototoxicity by changing the cell death mechanism from apoptosis to pyroptosis. *J Photochem Photobiol B*. 2016;161:177–83.
51. Andrew P, Voigt, et al. Single-cell transcriptomics of the human retinal pigment epithelium and choroid in health and macular degeneration. *Proc Natl Acad Sci U S A*; 2019.
52. Joseph C, et al. Single-cell RNA sequencing reveals transcriptional changes of human choroidal and retinal pigment epithelium cells during fetal development, in healthy adult and intermediate age-related macular degeneration. *Hum Mol Genet*; 2023.
53. John V, Forrester, Heping, Xu. Good news-bad news: the Yin and Yang of immune privilege in the eye. *Front Immunol*, 2012.

Publisher's note

Springer Nature remains neutral with regard to jurisdictional claims in published maps and institutional affiliations.